

tering which they would yield with these experimental results. From the standpoint of naïve statistical mechanical theories of liquid structure, some of them seem at least equally plausible with the droplet model, particularly when the

extremely small size of droplet demanded is taken into account.

The author is indebted to Professor Gingrich and Professor Eisenstein for helpful conversations.

PHYSICAL REVIEW

VOLUME 74, NUMBER 9

NOVEMBER 1, 1948

A Study of Cosmic-Ray Bursts

H. S. BRIDGE, W. E. HAZEN,* B. ROSSI, AND R. W. WILLIAMS

Physics Department and Laboratory for Nuclear Science and Engineering, Massachusetts Institute of Technology, Cambridge, Massachusetts

(Received June 21, 1948)

A "fast" ionization chamber, suitable for the investigation of cosmic-ray bursts, is described. The operation of the chamber and of the associated electronic circuits is discussed. The nature of the cosmic-ray events responsible for the production of ionization bursts was studied (*a*) by observing coincidences between several ionization chambers, (*b*) by analyzing the shape of the ionization pulses, (*c*) by operating an ionization chamber inside a cloud chamber which was expanded whenever the ionization chamber recorded a pulse. The experimental results led to the following conclusions: (1) at mountain altitudes

98 percent of the ionization pulses in an unshielded chamber of the type used are produced by nuclear disintegrations, the remaining 2 percent by air showers; (2) in the nuclear disintegrations, heavily ionizing particles of sufficiently high energy are produced to cause coincidences between neighboring chambers; (3) nuclear disintegrations are produced mainly by non-ionizing rays, which are possibly neutrons, certainly not photons; (4) about 12 inches of lead is necessary to reduce the intensity of the radiation which produces nuclear disintegrations to $1/e$ times its original value.

I. INTRODUCTION

THE ionization chamber has been widely used in cosmic-ray studies, both as an *integrating instrument*, to record the average number of ion pairs per second produced by cosmic rays in a given volume of gas, and as a *pulse instrument*, to detect the sudden appearance of large "bursts" of ionization. The most common cosmic-ray phenomena which give rise to ionization bursts are (*a*) *cascade processes* (initiated by high energy electrons or photons) resulting in the production of large electron showers, (*b*) *nuclear disintegrations* resulting in the emission of one or more heavily ionizing particles, mostly protons and α -particles with energies of the order of 10^6 or 10^7 ev. Recent experiments have brought to light the existence of complex reactions in which showers and heavily ionizing particles appear simultaneously.

The advances in experimental techniques made during the war at the Los Alamos Labora-

tories and elsewhere have opened a wider field of application for the ionization chamber as a pulse instrument.¹ It has been shown that by using improved electronic circuits and by taking appropriate precautions to prevent electron attachment, ionization chambers can be made into detectors which are considerably faster and more sensitive than ionization chambers of the older type. It has thus become possible to use ionization chambers for a greater variety of experiments, in particular for coincidence experiments in which small resolving times are required.

Experiments on cosmic rays by means of "fast" ionization chambers were begun at the Massachusetts Institute of Technology in the spring of 1946. Preliminary reports on some of the results obtained have already been published.²⁻⁸ The present paper discusses methods

* Now at the University of Michigan, Ann Arbor, Michigan.

¹ See "Ionization chambers and counters" by B. Rossi and H. S. Staub, Vol. 2 of the Los Alamos Technical Series, in press. This work will be referred to as R.S.

² H. Bridge and B. Rossi, Phys. Rev. 71, 379 (1947).

³ H. Bridge, Phys. Rev. 72, 172 (1947).

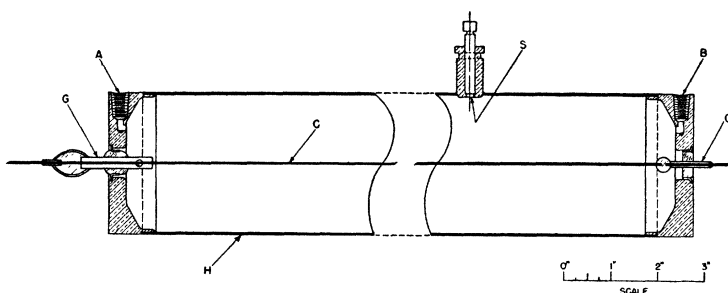


FIG. 1. The ionization chamber.

for separating the various kinds of cosmic-ray events which produce bursts in ionization chambers and describes some new results concerning cosmic-ray-induced nuclear disintegrations. These results were obtained by means of ionization chambers used both alone and in conjunction with a cloud chamber.

II. THE IONIZATION CHAMBER AND AMPLIFIER

1. Design and Electric Connections of the Chamber

All of the chambers used in our experiments were of cylindrical shape and similar in design to the chamber described in R.S., Chap. 5.4. The constructional details were somewhat modified in the course of the work and Fig. 1 represents the design which was adopted in the most recent experiments.

The outer shell *H*, which is also the high voltage electrode, consists of a brass tube 3 inches in outer diameter with $\frac{1}{32}$ -inch walls. The collecting electrode, *C*, is a kovar wire, 0.025 inch in diameter and $20\frac{1}{8}$ -inch effective length stretched along the axis of the brass tube. This wire is supported by the glass-kovar seals shown in the figure. The kovar cylinders, *G*, (guard electrodes) are grounded during operation to

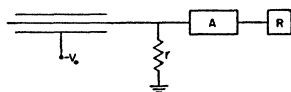


FIG. 2. Electrical connections of the ionization chamber.

⁴ B. Rossi and R. W. Williams, Phys. Rev. **72**, 172(A) (1947).

⁵ R. W. Williams and B. Rossi, Phys. Rev. **72**, 172(A) (1947).

⁶ H. Bridge, B. Rossi, and R. W. Williams, Phys. Rev. **72**, 257 (1947).

⁷ H. Bridge, W. E. Hazen, B. Rossi, Phys. Rev. **73**, 179 (1948).

⁸ R. W. Williams, Phys. Rev. **73**, 1252 (1948).

prevent leakage of charges from the high voltage electrode to the collecting electrode. *S* represents a polonium source, which is used for the calibration of the chamber. *A*, *B* are the connections for the gas filling (see below).

The electrical connections of the chamber are schematically represented in Fig. 2. The outer shell is kept at a fixed negative voltage $-V_0$ of the order of 1500 volts. The collecting electrode is grounded through a resistor, *r*, and connected to the input of an electronic amplifier, *A*. The output of the amplifier feeds into a recorder, *R*, which may be either a cathode-ray oscilloscope or an electronic pulse height discriminator. The combined capacity to ground, *C*, of the collecting electrode, the amplifier input and the connecting leads will be called the "input capacity." The product *RC* will be referred to as the "input time constant."

2. Operation of the Chamber⁹

In this section we shall discuss the relationship between the number and distribution of ion pairs produced in the chamber by a given ionizing event, and the size and shape of the corresponding voltage pulse at the output of the amplifier. The chamber is filled with argon, a gas in which no electron attachment takes place, so that the negative ions are free electrons (see Section 3 below). The operation of the chamber can be described by considering it as a generator whose output current, *I*, depends on the ionization of the gas. The expression for *I* may be written as $I = I^+ + I^-$ where I^+ and I^- are given by the equations:

$$I^+ = (e/V_0)[\sum w_i^+ E_i^+]; \quad I^- = (e/V_0)[\sum w_i^- E_i^-], \quad (1)$$

In the above equations, *e* represents the electronic charge; V_0 , the voltage difference between

⁹ See reference 1, Chap. 3.

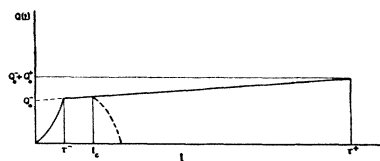


FIG. 3. Charge displaced through the ionization chamber as a function of time (schematic).

the electrodes; w_i^+ , the drift velocity of a given positive ion; E_i^+ , the electric field strength at the place where this ion finds itself at the time considered. The corresponding quantities for a given electron are w_i^- , E_i^- . The summations are extended to all of the ions and electrons present in the chamber. I^+ and I^- may be considered to represent the contributions of the motion of positive ions and electrons respectively, to the total intensity, I , of the ionization current.

Consider the case that N ion pairs are produced simultaneously in the chamber at the time $t=0$. An ionization current will set in and last until all ions have been collected. Under the conditions of our experiments, the drift velocity of the electrons is of the order of 10^6 cm sec.⁻¹, the drift velocity of positive ions is of the order of 10^3 cm sec.⁻¹. Therefore the electron current I^- will last for a time τ^- of the order of microseconds, while the positive ion current I^+ will last for a time τ^+ about 1000 times longer and will have a value correspondingly smaller. It follows that the charge displaced through the chamber at the end of time t , i.e., the quantity

$$Q(t) = \int_0^t I(t_1) dt_1$$

increases at first very rapidly until all electrons have been collected ($t=\tau^-$) and then much more slowly, until the collection of the positive ions is completed ($t=\tau^+$) as shown schematically by the solid line in Fig. 3.

Let us indicate with Q_0^- and Q_0^+ the total charges induced by the motion of electrons and positive ions, respectively. Integration of Eqs. (1) yields

$$\begin{aligned} Q_0^- &= -(e/V_0) \left[\sum_1^N V_i \right], \\ Q_0^+ &= (e/V_0) \left[\sum_1^N (V_i - V_0) \right], \\ Q_0 &= Q_0^+ + Q_0^- = Ne, \end{aligned} \quad (2)$$

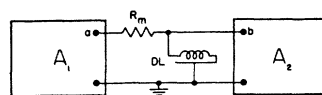


FIG. 4. Schematic diagram of "delay line clipping."

where V_i is the voltage at the place where the i th ion pair is produced. Since the charge induced by the motion of the positive ions in the time τ^- is negligible compared with the charge induced by the motion of the electrons in the same time, the value of Q at $t=\tau^-$ is practically identical with Q_0^- .

The electronic amplifiers used in our experiments were of the type described as "model 100 Amplifiers" in Vol. I of the Los Alamos Technical Series by W. C. Elmore and M. Sands, and were equipped with a "delay-line" type of low frequency rejection network (or "delay line clipping"). This device consists of a delay line DL in series with its matching resistor R_m , and is inserted between two sections A_1 , A_2 of the amplifier, as shown in Fig. 4, where a is the output of the first section of the amplifier and b the input of the second section. The output impedance at point a is very small compared to the characteristic impedance of the delay line. Hence the first reflected pulse is absorbed in R_m with no further reflections. Thus, the voltage at b is the superposition of two voltage pulses; a direct pulse of the same shape as the pulse at a and a reflected pulse of opposite sign delayed by a time t_e equal to twice the delay time of the line. If the delay line has no attenuation, both of these pulses have amplitudes equal to one half the amplitude of the pulse at a . If all coupling time constants (including the input time constant, RC) are long compared with t_e , the "transient response" of an amplifier with delay line clipping is of the general type shown in Fig. 5. The transient response is here defined as the function

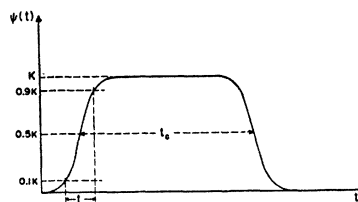


FIG. 5. Transient response of an amplifier with delay line clipping.

$\psi(t)$ which represents the output voltage obtained when a unit charge is applied instantaneously to the input at the time $t=0$. The maximum value, K , of the function $\psi(t)$ multiplied by the input capacity, C , may be defined as the "amplification" A :

$$A = KC. \quad (3)$$

The time t_r during which $\psi(t)$ rises from $0.1K$ to $0.9K$ will be referred to as the "rise time." The time t_c defined above will be referred to as the "clipping time."

The voltage at the output of the amplifier corresponding to an arbitrary current $I(t)$ at the input is given by the equation

$$V(t) = \int_{-\infty}^t I(t_1)\psi(t-t_1)dt_1. \quad (4)$$

In our experiments, the rise time t_r was short compared with the collection time of the electrons, τ^- , while the clipping time t_c was only slightly longer than τ^- and, therefore, was very short compared with the collection time of positive ions τ^+ . Under these conditions the computation of the output voltage corresponding to an ionization burst at $t=0$ can be simplified by considering $\psi(t)$ a square wave, i.e., by taking $\psi(t) = K = \text{const.}$ for $0 < t < t_c$ and $\psi(t) = 0$ for $t < 0$

or $t > t_c$. Equation (4) then yields:

$$V(t) = K \int_0^t I(t_1)dt_1 = KQ(t) \quad \text{for } t < t_c, \quad (5)$$

$$V(t) = K \int_{t-t_c}^t I(t_1)dt_1 = K[Q(t) - Q(t-t_c)] \quad \text{for } t > t_c.$$

These equations together with Fig. 3 show that $V(t)$ reaches the value KQ_0^- at $t = \tau^-$, stays practically constant until $t = t_c$ and then decreases again, reaching zero at the time $t_c + \tau^-$, as indicated by the dotted curve in the same figure. Thus the size of the input pulse is proportional to the charge Q_0^- induced by the motion of the electrons.

The value of Q_0^- depends on the number, N , of ion pairs produced in the chamber and on the position in which these ions are produced (see Eq. (2)). For instance, if N ion pairs are produced at the same distance r from the axis of the chamber, Q_0^- has the value

$$Q_0^- = Ne[\ln(r/a)/\ln(b/a)], \quad (6)$$

where a is the radius of the wire, b the radius of the outer cylinder. If, instead, the ionization is distributed uniformly throughout the chamber we obtain:

$$Q_0^- = Ne[b^2/(b^2 - a^2) - 1/2 \ln(b/a)] \quad (7)$$

or, for a chamber of the dimensions specified in Section II-1, $Q_0^- = 0.90Ne$. Consider finally the case of a particle with constant specific ionization which traverses the chamber perpendicular to the axis, at a distance r from it. Curves giving Q_0^-/Ne vs. r/b are shown in Fig. 6 for different values of the ratio b/a . Ne is the total charge which would be released by a particle intersecting the axis ($r=0$) if a were equal to zero. The variation of the induced charge, Q_0^- , with increasing r shown by the curves in Fig. 6 is the result of two effects which act in opposite directions, namely, the reduction in the length of the track and the increase in its distance from the collecting electrode.

3. Gas Filling

An attempt was made to use mixtures of argon and CO_2 as gas filling in order to obtain

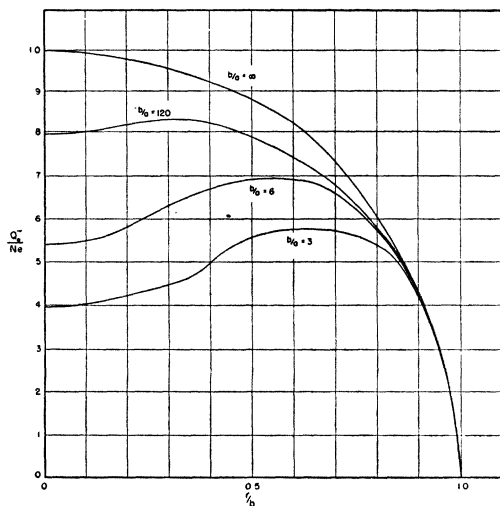


FIG. 6. Size of the electron pulse for a particle traversing the ionization chamber perpendicularly to the axis, as a function of the distance r of the track from the axis.

very short times of collection for electrons (see R.S., Chap. 1.4). The experience at Los Alamos has shown that chambers of a design similar to ours work satisfactorily with argon—CO₂ filling as detectors for γ - or β -rays (see R.S., Chap. 5.4). In testing the chambers with a source of polonium α -particles, however, it was found that the size of the pulses obtained with 5 atmospheres of argon plus 5 percent of CO₂ varied as the voltage across the chamber was changed and failed to reach saturation at the maximum voltage allowed by the design of the instrument. We believe that the reason for this behavior is columnar recombination, the influence of which is negligible in the case of lightly ionizing rays such as high energy electrons, but becomes important in the case of heavily ionizing rays such as α -particles. Since it was desirable to obtain quantitative response both for lightly ionizing and for heavily ionizing particles, and to use fairly high pressures so as to increase the sensitivity of the chamber, an effort was made to minimize columnar recombination by a more appropriate choice of the gas. It was found that pure argon with pressures up to about 7 atmospheres behaves satisfactorily in this respect and pure argon filling was thus adopted in all of our experiments. With 5 atmospheres pressure and 1000 to 2000 volts across the chamber, the time of collection of electrons was found to be approximately 7 microseconds. This time, even though considerably longer than the collection time in argon—CO₂ mixtures (see R.S., Chap. 5.4), proved adequate for most of our applications.

The filling procedure was as follows: the chamber was connected at *A* and *B* (see Fig. 1) to a purifier, consisting of an iron vessel filled with calcium metal chips, which could be heated electrically. The chamber and the purifier were first kept under vacuum for several hours with the purifier at 300°C. Then they were filled with tank argon through a dry ice trap. After closing the connection with the filling system, the gas was allowed to circulate by convection through the purifier at 300°C for 12 hours, at the end of which period the chamber was sealed off from the purifier.

4. Calibration

For the calibration of the chambers and of the amplifiers two different methods were used.

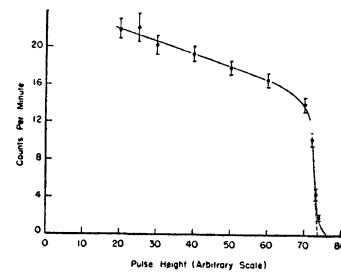


FIG. 7. Bias curve obtained with a polonium source in the chamber.

(a) As already mentioned, all chambers were provided with a polonium source placed near the outer wall. The polonium α -particles have an energy of 5.3 Mev and their range in argon at 5 atmospheres (the smallest pressure used in our chambers) is 0.74 cm. This range is small compared with the radius of the chamber. The α -particles brought to rest in the gas produce a number of ion pairs given by $N = 5.3 \times 10^6 / W_0$, where W_0 is the average energy to produce an ion pair, which, for argon, is equal to 26 ev. Since the range of the α -particles is small compared with the radius of the chamber, the corresponding value of Q_0^- depends only slightly on the direction of the track. It is a maximum for a track running close to the wall, in which case $Q_0^- = Ne = 2.04 \times 10^5 e$, and is 3 percent smaller than this maximum for a track perpendicular to the wall. The most convenient way to determine the maximum pulse height is to find the end point of the integral pulse height distribution, or *bias curve*, i.e., of the curve which gives the number of pulses larger than a certain size as a function of this size. As an example, the bias curve obtained with one of our ionization chambers is shown in Fig. 7. Its end point is determined by extrapolation of the linear portion of the curve, as shown in the figure. In the arbitrary scale of pulse height used, the extrapolated end point is at $P = 74$. In this experiment, the voltage across the chamber was 675 volts. No appreciable change in the bias curve was observed by raising the voltage from 675 to 2000 volts. This may be taken as an indication that already at 675 volts electron recombination and attachment were negligible. In other chambers this condition was reached at a somewhat larger voltage, which, however, was never higher than 800 volts. The bias curve shown in Fig. 7 was

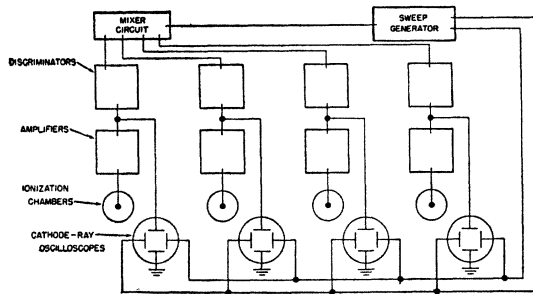


FIG. 8. Block diagram of the electronic equipment used in the coincidence experiments.

measured at sea level, where the cosmic-ray background is negligible compared with the counting rate from the polonium α -particles as shown by the fact that practically no counts are recorded at a bias slightly larger than the α -particle end point. The lack of a flat "plateau" in the bias curve is presumably explained by a background of pulses from radioactive contamination of the chamber. This background does not affect appreciably the extrapolated end point of the polonium α -particles.

(b) An electronic pulser was built to apply voltage pulses of known magnitude and in the shape of step functions to the high voltage electrode of the chamber. The charge Q_1 induced on the collecting electrode when the potential of the high voltage electrode is changed by a value V_1 is given by

$$Q_1 = C_1 V_1,$$

where C_1 represents the capacity between the two electrodes of the chamber. C_1 can be calculated easily if end effects are neglected. For a chamber of our type the calculated value of C_1 is $6.1 \mu\mu\text{F}$. The extrapolated end points of the α -particle bias curve were found to be within 20



FIG. 9. Photographic record of the four horizontal traces of the coincidence method. The apparatus was triggered by the large pulse appearing on the right-hand trace; two other traces show small time-coincident pulses.

percent of the value computed from the calibration by means of artificial pulses. It is believed that the uncertainties in the energy loss per ion pair, W_0 , and in the value of the interelectrode capacity, C_1 , are sufficient to account for the discrepancy. In what follows, the calibration of the chambers will be based on the bias curves of the polonium α -particles. Pulse heights will be measured by the quantity $Q_0^- W_0/e$ expressed in electron-volts. This quantity represents the energy dissipated in the production of Q_0^-/e ion pairs.

III. COINCIDENCE EXPERIMENTS

1. The Principle of the Method

Ionization bursts caused by showers and by heavily ionizing particles can be separated by using several ionization chambers properly arranged and by recording the pulses of the various chambers simultaneously. Both the probability of a coincidence between the chamber pulses, and the distribution in size of the pulses when a coincidence occurs, are different depending on whether the chambers are recording showers or nuclear disintegrations.

2. The Experimental Equipment

In the coincidence experiments, four ionization chambers were used. A block diagram of the electronic equipment is shown in Fig. 8. The pulses of the individual chambers were amplified separately and brought to the deflecting plates of four cathode-ray oscilloscopes. The same pulses were also brought to four pulse height discriminators which could be adjusted to fire for signals larger than a predetermined value. The output pulses of the four discriminators were fed to a mixer circuit, which gave a pulse whenever at least one discriminator fired. This pulse was used to trigger a sweep generator, the purpose of which was to intensify the beams of the oscilloscopes (which were normally biased below cut-off) and to provide a linear horizontal sweep. The four oscilloscope screens were photographed on a continuously moving film. Figure 9 is the reproduction of a picture showing pulses of different sizes in three of the four chambers and no pulse in the fourth.

The equipment was calibrated at frequent

intervals during the experiments, both with α -particle pulses and with artificial pulses. The gain was adjusted so that the minimum detectable deflection of the oscilloscope beams corresponded to a pulse of 0.25 Mev. This size of pulse was about ten times larger than the (r.m.s.) amplifier noise. Pulses caused by electric pick-up were occasionally recorded but could be easily distinguished from ionization pulses by their oscillatory nature. They were, of course, rejected in the evaluation of the data. The speed of the sweep was 7×10^4 cm sec.⁻¹ and its total duration 60 microseconds. Examination of the oscilloscope records made it possible to establish the simultaneity of the pulses in the various chambers with an accuracy of 6 microseconds.

3. Separation of Bursts from Showers and Nuclear Disintegrations

The four chambers were arranged close to one another with their axes horizontal, as shown in Fig. 10. The group of chambers was enclosed in a wooden box $\frac{1}{4}$ -inch thick, lined with a 0.011-inch copper sheet for electrostatic shielding. The box was placed in a wooden shack at Climax, Colorado (elevation 3500 meters, average atmospheric pressure 673 g cm⁻²). The roof of the shack was 1.5 g cm⁻² thick. Measurements were taken with the circuit adjusted to trigger the four sweeps whenever a pulse larger than 7.5 Mev appeared in any one of the four chambers. Such a pulse is 1.4 times the pulse produced by a polonium α -particle and consequently we may assume that only cosmic-ray events were recorded. The fact that the rate of occurrence of pulses larger than 7.5 Mev increases by a factor of about 14 between sea level and 3500 meters conclusively confirms our assumption. The results obtained in 63.1 hours of observation are summarized in Table I, and parts of these data are analyzed in Figs. 11, 12, and 13. Table I gives a classification of the pulses larger than 7.5 Mev which occurred in chamber 2 or in chamber 4 according to whether pulses larger than 0.25 Mev occurred simultaneously in none, one, two, or three of the other chambers. Curve (a) in Fig. 11 shows the combined integral pulse height distribution for the pulses of chamber 2 which *are not* accompanied by pulses larger than 0.25 Mev in chambers 1, 3, 4, and for the pulses of chamber

TABLE I. Classification of the pulses larger than 7.5 Mev in chamber 2 (the upper chamber) and chamber 4 (the lower chamber) according to the number *N* of *additional* chambers in which simultaneous pulses larger than 0.25 Mev occurred.

Chamber	2				4			
<i>N</i>	0	1	2	3	0	1	2	3
Total counts	644	130	35	21	733	87	21	28
Counts per hour	10.2	2.06	0.55	0.33	11.6	1.38	0.33	0.44

4 which *are not* accompanied by pulses larger than 0.25 Mev in chambers 1, 2, 3. Similarly, curve (b) in the same figure shows the combined integral pulse height distribution for the pulses of chamber 2 or chamber 4 which *are* accompanied by a pulse larger than 0.25 Mev in at least one other chamber.

Figure 12 is a histogram of the frequency of occurrence of various values of the mean deviation from the mean of pulse heights in events in which three chambers had observable pulses. These mean deviations have been divided by the square root of the mean, in order that events with different mean pulse heights may be com-

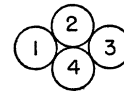


FIG. 10. First arrangement of the chambers in the coincidence experiments.

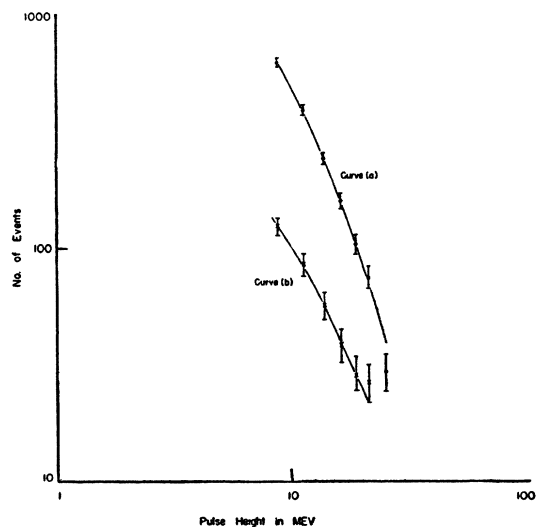


FIG. 11. Integral pulse height distributions for single pulses (curve a) and for coincidences (curve b) (time of observation 35.7 hours).

pared. The quantity plotted is therefore

$$x = \sum_{i=1}^3 \frac{|(P)_{Av} - P_i|}{3((P)_{Av})^{\frac{1}{2}}}$$

where P_i is the pulse height in the i th chamber, and $(P)_{Av}$ is the average pulse height for the three chambers.

Figure 13 shows the same type of histogram for fourfold coincidences.¹⁰

In the experiment described, no heavy material was present above the chamber. This rules out the possibility that locally produced ordinary cascade showers may be partly responsible for the observed bursts. These bursts, therefore, must be produced either by large air showers or by nuclear interactions. It is reasonable to assume that an air shower should produce pulses of not very different sizes in the four thin-walled chambers used in our experiments. Direct experiments fully confirm this view, as will be shown in a separate paper by R. W. Williams. Thus any event in which at least one of the ionization chambers fails to give a detectable pulse must be interpreted as the result of nuclear interactions. Indeed it is likely that not even all of the fourfold coincidences are caused by air showers. Examination of Fig. 13 shows that the

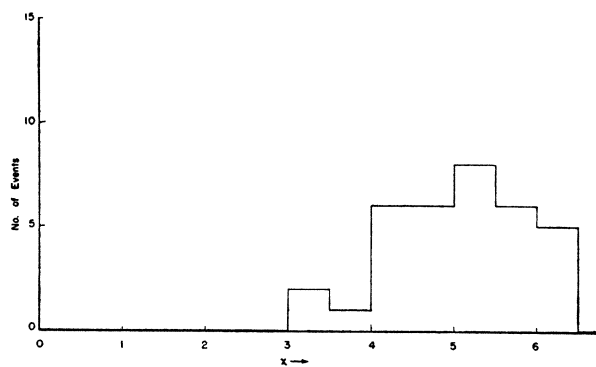


FIG. 12. Spread in pulse height for threefold coincidences.

¹⁰ Qualitative examination of the records shows that the fourfold events fall into two groups, "large-deviation" and "small-deviation" events. When the chambers are struck by an air shower we would expect a small mean deviation, caused mainly by the fluctuations in the number, N , of particles traversing each chamber. The distribution in number of particles may approximate a Poisson distribution, for which, if $(N)_{Av}$ is large, the mean deviations are proportional to $((N)_{Av})^{\frac{1}{2}}$. Therefore, if we divide by $((P)_{Av})^{\frac{1}{2}}$, which is proportional to $((N)_{Av})^{\frac{1}{2}}$, we will compare all air showers on the same basis, regardless of size.

fourfold coincidences fall rather sharply into two groups, one in which the mean deviations are small, and one in which the mean deviations are large. It is natural to explain the pulses of the first group as caused by air showers, the pulses of the second group as caused by nuclear disintegrations. One thus concludes that air showers and nuclear disintegrations account, respectively, for 55 percent and 45 percent of the fourfold coincidences observed. It appears that very few of the ionization pulses observed at 3500 meters in thin-walled ionization chambers of our type are produced by air showers. The total number of pulses larger than 7.5 Mev in each chamber, regardless of whether or not detectable pulses were present in any other chamber, was 13.45 per hour. Of these, 0.3 per hour were accompanied by pulses of size comparable with their own in all of the other chambers. Thus air showers contribute about 2 percent of the total number of pulses larger than 7.5 Mev observed in a single chamber.

It should be noted that the relative numbers of pulses produced by air showers and by nuclear disintegrations is dependent on the dimensions of the chamber, the pressure of the gas, and the bias setting. It was found, for instance, that at 3500 meters the number of pulses larger than a certain size P produced by air showers varies as $P^{-1.7}$.^{8,11} As shown in Fig. 11, the pulse height distribution for all pulses decreases more rapidly with increasing P . It thus follows that the contribution of air showers relative to that of nuclear disintegrations becomes increasingly important

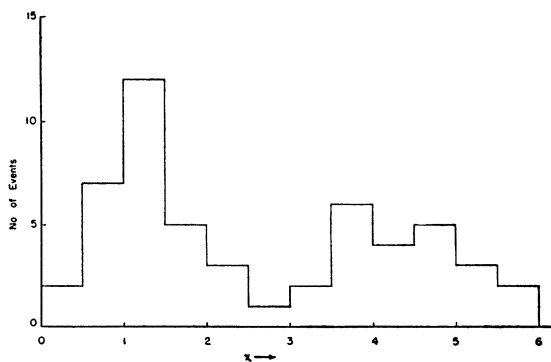


FIG. 13. Spread in pulse height for fourfold coincidences.

¹¹ R. W. Williams, to be published.

as the bias energy is raised. The pulse height distribution which we observe also verifies the interpretation given for Carmichael's burst data by H. Euler.¹² Also, because of the relatively short range of the fragments from nuclear disintegrations and the large range of shower electrons, high gas pressure favors the detection of air showers. Thus Lapp,¹³ whose ionization chamber had a pressure of fifty atmospheres, and who required an energy loss of several hundred Mev, reports that about 85 percent of his bursts at sea level were caused by air showers.

4. Further Results Concerning Nuclear Disintegrations

An unexpected result of our experiments was the fairly large number of coincidences between neighboring ion chambers which arise from nuclear events. It is believed that most of these events are disintegrations which take place in the wall of one chamber, and in which protons of sufficiently high energy to penetrate the walls of other chambers are produced. It may be noted that a proton must possess at least 21-Mev energy to traverse one chamber wall and 31 Mev to traverse two chamber walls. On the other hand, any proton with more than 0.25 Mev and less than 230 Mev traversing a chamber along a diameter will produce a detectable pulse. The large spread in size of the pulses simultaneously produced in two or more chambers by nuclear interactions (see Figs. 12, 13) is consistent with this interpretation.

Measurements were made of the coincidence rate between two chambers in contact as a function of their relative position. It was found that this rate is practically the same when the chambers are arranged one above the other and when they are arranged one beside the other. This result is again consistent with the above interpretation, since it is known that the heavily ionizing particles produced in nuclear interactions are distributed *approximately* at random in direction. However, the data in Table I clearly indicate a slight tendency for these particles to be projected in a downward direction. In fact, while the total counting rate for pulses larger

TABLE II. Number of coincidences in 42.2 hours between the different pairs of chambers in Fig. 14.

Chambers	Distance between axes (inches)	Coincidences in 42.2 hours
1, 2	3	66
2, 3	4½	39
3, 4	6	32
1, 3	7½	18
1, 4	13½	8

than 7.5 Mev is very closely the same for chambers 2 and 4 (13.1 and 13.7 respectively), the fraction of such pulses accompanied by pulses in other chambers is greater for chamber 2 (upper chamber).

The coincidence rate was also measured as a function of the distance between chambers. For this experiment the four chambers were arranged with their axes in a horizontal plane, as shown in Fig. 14. The numbers of coincidences recorded in 42.2 hours are shown in Table II. It is seen that the number of coincidences decreases very rapidly with increasing distance. An approximate calculation shows that this number varies roughly as the average solid angle subtended by one chamber at the other, as one would expect according to our interpretation. It is possible, of course, that the rate of coincidences (1, 3) and (1, 4) might be reduced by absorption in the walls of the intervening chambers. Even though there seems to be little doubt that most of the coincidences are caused by single nuclear events, the possibility cannot be excluded that some coincidences may be produced by two or more disintegrations occurring simultaneously in different ionization chambers.

In order to obtain information on the nature of the radiation which causes the observed disintegrations, measurements were taken with the chambers arranged as shown in Fig. 10 and with lead absorbers of different thicknesses placed around them (see Fig. 15). The results obtained are summarized in Fig. 16, where the abscissa represents the thickness in g cm⁻² of the lead

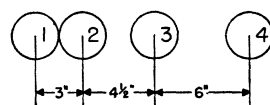


Fig. 14. Arrangement of chambers for the study of the variation of the coincidence rate with distance.

¹² H. Euler, Zeits. f. Physik 116, 73 (1940). See also J. Clay and C. G. T'Hooft, Physica 9, 251 (1944).

¹³ R. E. Lapp, Phys. Rev. 69, 321 (1946).

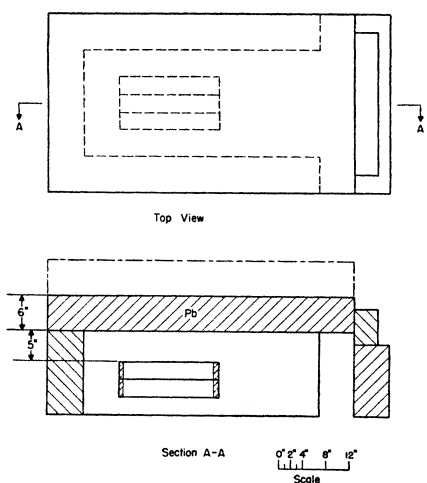


FIG. 15. Arrangement of ionization chambers and lead shields for the absorption measurements with 6 inches of lead. Dashed line in sectional view shows the additional 6 inches used for the 344 g cm^{-2} point.

absorber and the ordinate represents the corresponding transmission; i.e., the ratio N/N_0 of the counting rates with and without lead. It should be noted that in the measurements at 115 g cm^{-2} and 172 g cm^{-2} the thickness of lead on the sides was equal to that on top, while the point at 344 g cm^{-2} was obtained with only 172 g cm^{-2} on the sides.

Data for the following events were recorded: (a) a pulse larger than the bias energy in chamber 2 or 4 not accompanied by a pulse larger than 0.25 Mev in any other chamber; (b) a pulse larger than the bias energy in any chamber accompanied by pulses larger than 0.25 Mev in one or two additional chambers; (c) a pulse larger than the bias energy in any chamber accompanied by pulses larger than 0.25 Mev in all other chambers. The bias energy was 12.5 Mev for the point at 115 g cm^{-2} of lead, and 7.5 Mev for the other two points. Experiments showed that the pulse height distribution is not appreciably affected by the lead shielding so that the values of the transmission should be independent of bias. The events of type (a) observed either with or without lead are surely caused by nuclear disintegrations. Indeed, a shower from the lead may strike one of the lateral chambers (1 or 3) without striking any other chamber, but cannot strike one of the middle chambers (2 or 4) alone. The possibility that any appreciable number of

showers may strike chamber 2 and be absorbed in the chamber walls, thus failing to discharge chamber 4, is ruled out by the observation that, with as well as without lead, single pulses of chambers 4 are slightly more numerous than single pulses of chamber 2 rather than the other way around (the interpretation of this slight difference has been given above). Thus the variation with increasing lead thickness of the counting rate for single pulses in chamber 2 or 4 may be considered to represent the absorption in lead of the radiation which produces nuclear disintegrations. The experimental data seem to indicate that the absorption curve has an inflection point. We feel that further experiments are necessary before this detail may be considered as established beyond any doubt and before its possible significance may be profitably discussed. Here we only wish to point out that the absorption in lead of the parent radiation is much smaller than the absorption of high-energy electrons or photons. This result, which is in agreement with qualitative data obtained by the observation of "stars" in photographic emulsions,¹⁴ proves that electrons or photons are not the major source of nuclear disintegrations in cosmic rays. Our results are not in disagreement with the hypothesis that most of the disintegrations are produced by neutrons. The absorption curve for events of type (b) does not seem to

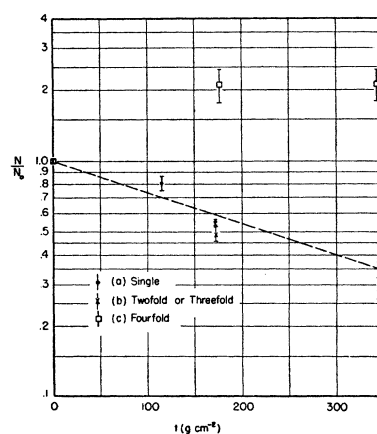


FIG. 16. Ratio of the counting rates with and without lead as a function of the lead thickness t . The straight line represents an exponential decrease with a mean free path of 330 g cm^{-2} .

¹⁴ D. H. Perkins, *Nature* **160**, 707 (1947).

differ greatly from that for events of type (a). This may be construed as an indication that, also under lead, twofold and threefold coincidences, as well as single pulses, are mainly caused by nuclear disintegrations.

The number of fourfold coincidences (event c) is found to increase by about a factor of 2 when 172 g cm⁻² of lead is placed above the chambers. This increase can easily be understood if electron showers capable of discharging the four chambers are produced in the lead by a penetrating radiation. This effect is known to occur.^{6, 7, 13, 15} The failure to observe a decrease in the fourfold counting rate when the lead thickness is increased from 172 to 344 g cm⁻² is somewhat surprising in the light of other results.¹⁶ Here again, however, we feel that more accurate experiments are needed before any conclusion can be reached.

IV. THE PULSE SHAPE METHOD

1. The Principle of the Method

Some information on the nature of the processes which give rise to bursts in ionization chambers can be obtained by examining the *shape* of the pulses. The ionization produced by a shower is fairly uniformly distributed over a large portion of the volume of the chamber, while the ionization caused by a nuclear disintegration is concentrated along the tracks of a few heavily ionizing particles. To the different distribution in space of the ionization there corresponds a different time dependence of the observed voltage pulse, $V(t)$.

It is not possible to determine theoretically the exact pulse shape corresponding to a given distribution of ionization because the dependence of the drift velocity of electrons, w^- , on the field strength E in our ionization chamber is not well known. This is due, in part, to the fact that the drift velocity of electrons in argon depends critically on the purity of the gas. However, it turns out that the shape of the function, $V(t)$, depends more critically on the distribution of the ionization than on the form of the function $w^-(E)$. This is borne out by an examination of Fig. 17. Curves a, b, c , in this figure were com-

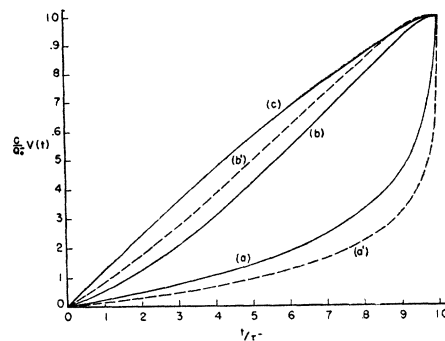


FIG. 17. Pulse shapes corresponding to different distributions of the ionization in the chamber, and to different relations between drift velocity and electric field strength.

puted under the assumption of a drift velocity independent of E for the following cases: (a) ionization confined to an infinitesimal layer adjacent to the chamber wall; (b) ionization uniformly distributed throughout the volume of the chamber; (c) ionization distributed uniformly along a straight line perpendicular to and passing through the axis of the chamber. The dotted curves a', b' in the same figure represent $V(t)$ for cases (a) and (b) respectively, computed under the assumption of a drift velocity proportional to the square root of the electric field strength.¹⁷

One sees that the qualitative character of curves a, a' , and b, b' respectively is essentially the same. The shape of the curves a, a' can be easily explained by considering that, under the assumptions made, all of the electrons at a given time are at the same distance from the axis of the chamber. They are, therefore, acted upon by

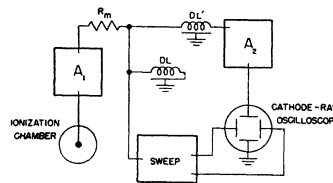


FIG. 18. Block diagram of the electronic equipment used for the analysis of pulse shapes. For significance of symbols see text and Fig. 4.

¹⁷ The actual dependence of w^- on E is complicated by the Ramsauer effect. $w^-(E) = \text{const.}$ is experimentally found to be approximately correct for large values of E , such as exist near the wire. $w^-(E) = \text{const.} \times E^{1/2}$ represents the drift velocity calculated under the assumptions that the mean free path for collisions is constant for all values of the agitation energy and that the energy loss of electrons is only caused by elastic collisions with the argon molecules.

¹⁵ W. B. Fretter, Phys. Rev. **73**, 41 (1948).
¹⁶ H. S. Bridge, as reported by B. Rossi, Rev. Mod. Phys. **20**, 537 (1948).

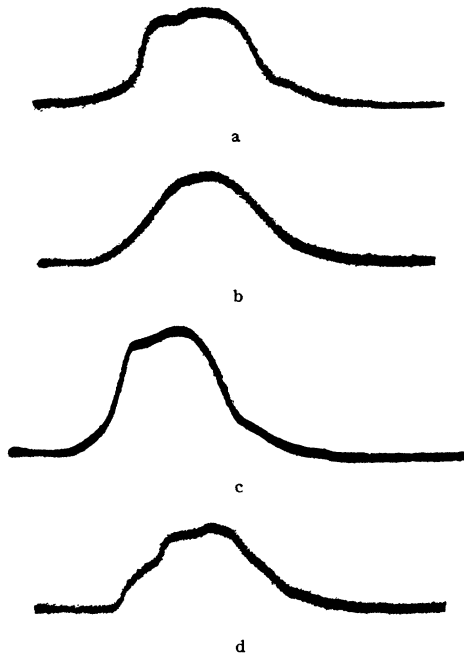


FIG. 19. Unshielded ion-chamber pulses (7500 meters). In some of the α - and ν -type pulses the negatives have been retouched so that the fast portion of the pulse rise can be reproduced satisfactorily. In all of the examples in this figure the pulses do not have an ideal flat top but show an additional rise at about $t_c/2$ which was later eliminated. (a) Pulse caused by P_0 - α -particle, (b) σ -type pulse caused by an air shower, (c) α -type pulse from nuclear disintegration, (d) ν -type pulse. This example shows a distinct break presumably caused by two particles one ending close to the wall and one close to the wire.

the same field strength, E , and have the same drift velocity, $w^-(E)$, so that Eqs. (1) yield:

$$CdV/dt = NeEw^-(E)/V_0, \quad (8)$$

where N is the total number of electrons. As the electrons drift toward the wire, E increases slowly at first, then very rapidly. The slope of the function $V(t)$ increases in proportion to E if $w^-(E)$ is constant and even more rapidly if $w^-(E)$ increases with E . The reader will find it easy to understand the physical reason for the shapes of the curves b , b' and c by considering how the initial distribution of the ionization affects the rate at which electrons arrive near the wire.

2. The Experimental Arrangement

A block diagram of the electronic equipment used for the analysis of pulse shapes is shown in Fig. 18.

The pulse of the chamber is applied to the

deflecting plates of the oscilloscope through a delay line, DL' , inserted at a point of the amplifier where the level of the signal is of the order of one volt. The undelayed pulse is further amplified and fed to a pulse height discriminator. The signal from the discriminator triggers the circuit which provides the intensifier pulse and the linear sweep for the oscilloscope. In this way it is possible to observe the beginning of the pulse despite the small inevitable delay in starting the sweep.

The line had a delay of 8.2 microseconds and its rise time was 0.3 microsecond. The oscilloscope screen was 5 inches in diameter and the sweep speeds used ranged from 2.5×10^5 to 5×10^5 cm sec. $^{-1}$. The pulse amplifier was of the type described in II.2. Its low frequency response was determined by "delay line clipping." Clipping times, t_c , between 10 and 15 microseconds were used.

3. Experimental Tests

The instrument described in the preceding section was first used to examine the shape of the α -particle pulses from the polonium source. This, as already mentioned (see II.1), was placed on the wall of the chamber. In argon at 5 atmospheres pressure, the range of a polonium α -particle is 0.74 cm and is therefore small compared with the radius of the chamber (3.75 cm). Thus the α -particle pulses should be of the general type represented by curves a and a' in Fig. 17. The experimental results were in agreement with these conclusions. All of the α -particle pulses were found to be very nearly of the same shape, showing an initial slow rise followed by a very fast one near the end of the pulse. An example of an α -particle pulse is reproduced in Fig. 19a.

In a second experiment, pulses arising from air showers were chosen by selecting events in which three Geiger-Mueller counters arranged in a horizontal plane were discharged simultaneously with the ionization chamber. The observations were carried out at 7500 meters in a B-29 aircraft. Altogether 5 air shower pulses were recorded. They all had approximately the same shape as the sample shown in Fig. 19b, in which one clearly recognizes the general character

predicted by the theory for uniformly distributed ionization (see Fig. 17, curves *b*, *b'*).

The pulses recorded with no auxiliary methods of identification had a variety of shapes, examples of which are shown in Figs. 19 and 20. A large fraction of the pulses had shapes very similar to that of an α -particle pulse (see Figs. 19c and 20b). Single heavily ionizing particles from nuclear disintegrations originating in the chamber wall and not passing close to the collecting wire probably account for most of these pulses, even though some of them may be caused by groups of short-range particles. Many examples were found of pulses showing two or more sharp "breaks" (see Fig. 19d). These correspond presumably to nuclear disintegrations which give rise to several heavily ionizing particles which stop in the gas at different distances from the wire. In some cases the slope of the pulse was greatest at the beginning and decreased gradually with increasing time (see, for instance, Fig. 20c). Comparison with Fig. 17 indicates that these pulses are probably caused by heavily ionizing particles passing near the wire. A few of the pulses observed with an unshielded chamber, and a large fraction of those observed under lead, had shapes indistinguishable from that of an air shower pulse (see Fig. 20a). It is likely, however, that not all of these pulses were actually produced by electron showers because a group of many heavily ionizing particles passing at different distances from the wire could produce a pulse practically indistinguishable from that of a shower. Further information bearing on the interpretation of pulse shapes will be presented in Part V.

For the sake of convenience, we shall adopt the following classification for the pulse shapes:

α -pulses: pulses with a single sharp break, resembling the pulses produced by the polonium α -particles.

σ -pulses: pulses with a smooth, almost linear rise, resembling those produced by air showers.

ν -pulses: pulses of all other shapes.

It must be noted that the exact boundary between σ and ν pulses is, to a certain extent, a matter of personal judgement.

Observations at 7500 meters with an unshielded chamber and with a chamber covered with 2.5 cm of lead gave the results shown in Table III.

TABLE III. Distribution of pulse shapes in an ionization chamber (a) unshielded, (b) under a 2.5-cm thick lead shield.

Pulse shape	(a) Percent of pulses	(b)
α	58	37
σ	16	44
ν	26	19

While all of the α -pulses and ν -pulses are probably produced by nuclear disintegrations, the discussion above suggests that not all of the σ -pulses are caused by showers. The pulse shape distribution in the unshielded chamber observed at 7500 meters altitude, therefore, cannot be taken as a proof that, at this altitude, the frequency of air showers relative to nuclear disintegrations is larger than 3500 meters, where it has been found to amount to 2 percent (see III.3).

V. OBSERVATIONS WITH A CLOUD CHAMBER EXPANDED BY PULSES FROM AN INTERNAL ION CHAMBER

1. The Experimental Method

In order to gain a more precise understanding of the nature of the cosmic-ray phenomena which are responsible for bursts in ionization chambers, and especially of those which give rise to coincidences between neighboring chambers, observations were made by means of a cloud chamber triggered by the pulses of an ionization

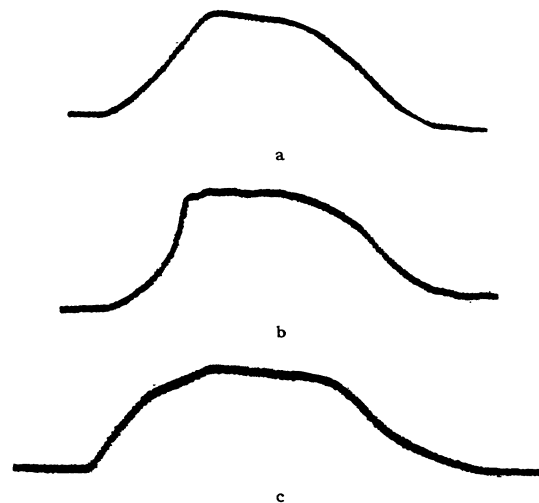


FIG. 20. Pulses from an ion chamber shielded by one inch of lead (sea level). (a) σ -type, (b) α -type, (c) ν -type showing a slope which decreases with time.

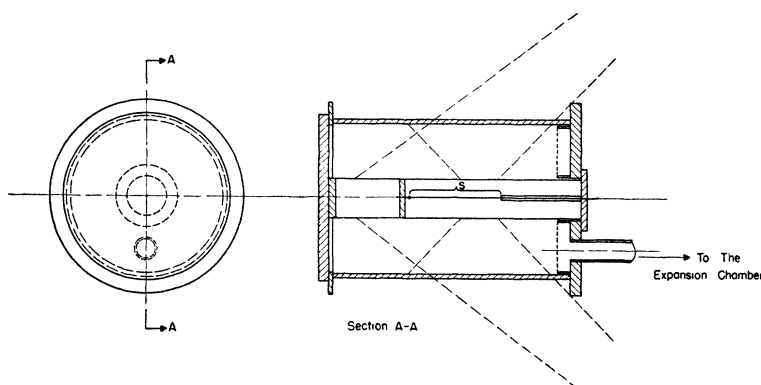


FIG. 21. Arrangement of ionization chamber inside the cloud chamber. The sensitive length of the ionization chamber wire is indicated by *S*. The approximate boundaries of the light beams are shown by the dashed lines; actually, of course, the boundaries are not sharp and it was found that heavily ionizing particles could be observed nearly anywhere in the chamber.

chamber built inside it. The diagram in Fig. 21 shows the essential features of the experimental arrangement. The ionization chamber was placed with its axis coincident with the axis of the cloud chamber. It was of the type described in Part II, except for modifications that made it suitable for insertion in the cloud chamber. The only significant modification was that one of the end plugs was seven inches from the sensitive volume whereas in the chambers of the usual type both end plugs are adjacent to the sensitive volume. The ionization chamber was 3 inches in diameter, the effective wire length was 7 inches. The walls were made of $\frac{1}{8}$ -inch-thick brass and the chamber was filled with argon at 5 atmospheres pressure.

The cloud chamber followed the general design of E. J. Williams¹⁸ in which the light scattered into the camera by the droplets is deflected through only 45 degrees. The resultant high brilliance of the droplets permits the photographic observation of a large depth of the cloud chamber. In addition, since track curvatures were not being measured, the droplet brilliance was enhanced by allowing a relatively long time for drop growth before taking the picture. Thus it proved feasible to observe the entire sensitive surface of an ionization chamber that was large enough to give a reasonable counting rate.

The expansion chamber was separated from the observation chamber in order to give free access to the terminals of the ionization chamber. It was found that, with any gas except hydrogen (i.e., with helium, argon, or air) the supersaturation threshold for formation of drops on

uncharged "condensation nuclei" was as low as (helium) or lower than the threshold for condensation on charged nuclei. Hence hydrogen was used as the permanent gas. All of the information leads to the conclusion that the two large chambers and their coupling tube resulted in an oscillatory pressure wave of sufficient amplitude to produce the observed effects.

Stereoscopic photography was used to demonstrate that all of the sensitive surface of the ionization chamber was within the observable region of the cloud chamber, and for spatial reconstruction of the tracks in all events of interest.

The electrical circuits associated with the ionization chamber were of the type described in Part II. Condenser coupling from the ionization chamber to the preamplifier allowed a high (positive) voltage to be applied to the collecting wire while the outer wall of the ionization chamber remained at ground potential. The observations were made with the discriminator adjusted to select pulses larger than about 6 Mev in the ionization chamber.

The instrument described was operated both at 3050 meters (Doolittle Ranch, Colorado), and at 4300 meters (Mt. Evans, Colorado). The data were taken partly with a $\frac{1}{4}$ -inch lead shield, in the shape of half a cylindrical shell, placed directly above and in contact with the ionization chamber, partly with lead plates of various thicknesses placed above the cloud chamber, partly with both lead shields, partly with neither of them. During some of the observations the pulses of the ionization chamber were recorded photographically as explained in Part IV.

¹⁸ E. J. Williams, Proc. Roy. Soc. A172, 206 (1939).

This made it possible to distinguish between pulses produced by ionization bursts and by electric pick-up from other equipment or from lightning, and to correlate the shape of the pulses in the ionization chamber with the events shown by the corresponding cloud-chamber records.

Examples of cloud pictures are shown in Fig. 22. Examples of correlated cloud-chamber

and ionization-chamber records are shown in Fig. 23.

2. Correlation of Ion-Chamber and Cloud-Chamber Records

The results of the observations in which the cloud-chamber and the pulse-recording equipment were operated simultaneously are summarized in Table IV. In the compilation of this

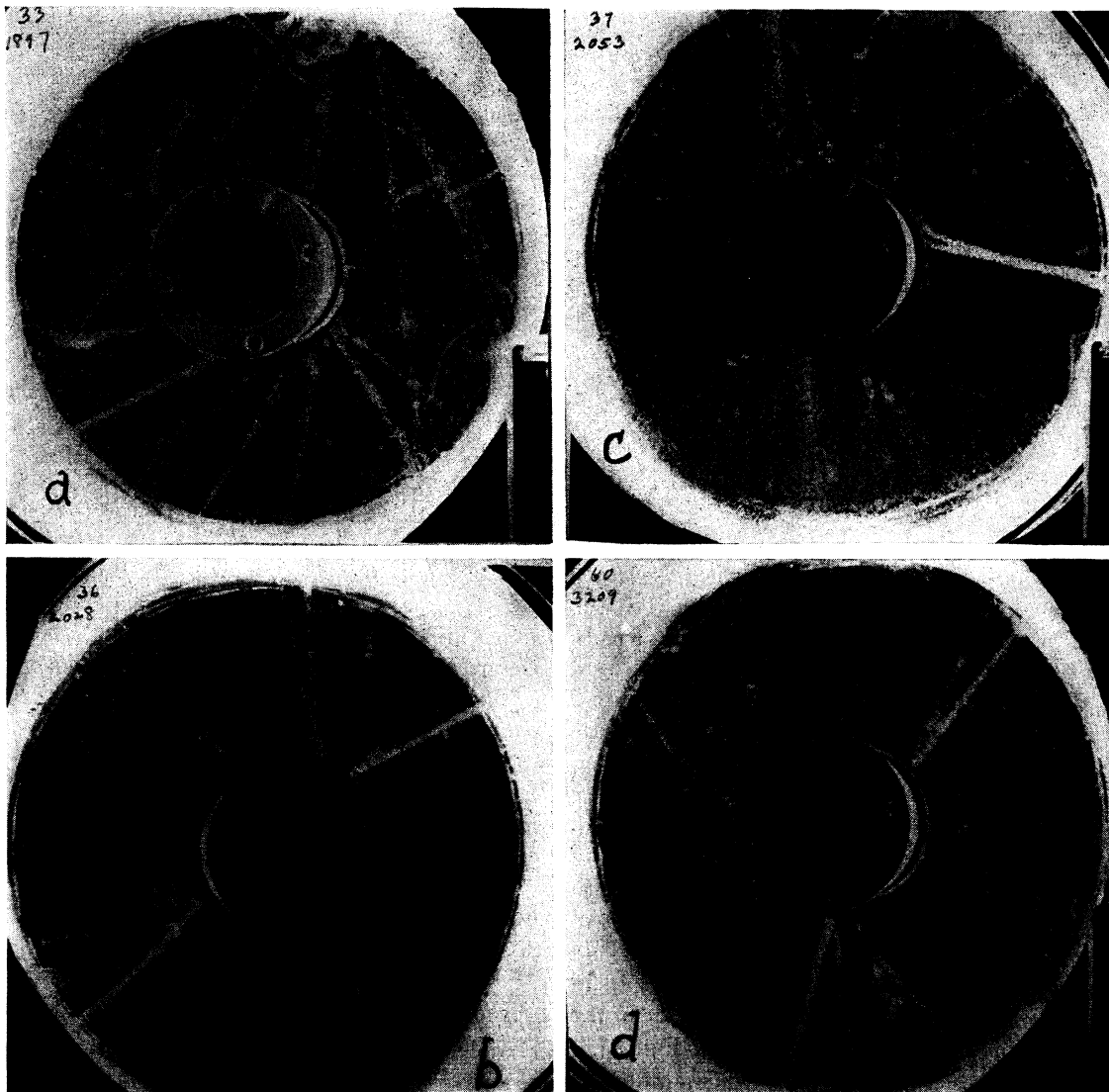


FIG. 22. Example of the cloud-chamber pictures. (a) An event in which a disintegration in the cloud-chamber wall is concurrent with a disintegration in the ionization-chamber wall. The latter may be initiated by a neutron from the former or both may be produced by neutrons from a disintegration above the apparatus. (b) A disintegration with four heavily ionizing and one lightly ionizing particles. (c) An electron shower from lead above the chamber apparently produces at least two heavy particles in a disintegration in the ionization-chamber wall. (d) A disintegration with at least seven particles appearing in the cloud chamber.



a



b

table, no distinction was made between data obtained with or without lead shielding. One will notice that in about 50 percent of the cases the cloud chamber does not show any track clearly associated with the event responsible for the burst in the ionization chamber. Since, as already pointed out, the illuminated volume of the cloud chamber completely surrounded the sensitive volume of the ionization chamber, these events presumably represent nuclear disintegrations in the gas or in the wall of the ionization chamber, in which no ionizing particles capable of penetrating the chamber wall are produced.

Table IV shows that the pulses associated with the 12 pictures of electron showers were all of the σ type. Most of these showers originated in the lead shield above the cloud chamber and in some cases the shower struck near the edge of the ionization chamber (see, for instance, Fig. 23e). It thus appears that showers produce pulses of the σ type even when they do not fill a major fraction of the ionization-chamber volume with uniform ionization. Of the 86 pulses which are attributed to nuclear disintegrations either because of the lack of associated tracks or

because of the appearance of heavily ionizing particles in the cloud-chamber picture, 80 have shapes of the α - or ν -type, 6 of the σ -type. One should finally note that some of the pulses of the ν -type appear to be caused by nuclear interactions in which heavily ionizing particles and electron showers are produced simultaneously.

The conclusion of this analysis is that electron showers are always recognized as such by the pulse shape but that a fraction of the order of 10 percent of the nuclear disintegrations give rise to pulses which simulate those produced by electron showers.

3. Relative Frequency of Showers and Nuclear Disintegrations Under Different Lead Shields

For this analysis, we consider all of the cloud-chamber pictures, whether or not simultaneous records of pulse shapes were obtained. The various types of events observed with different shieldings are listed in Table V. With no lead shielding, 55 pictures were obtained, of which only 3 showed electron showers and of these one showed an apparently time-associated heavy

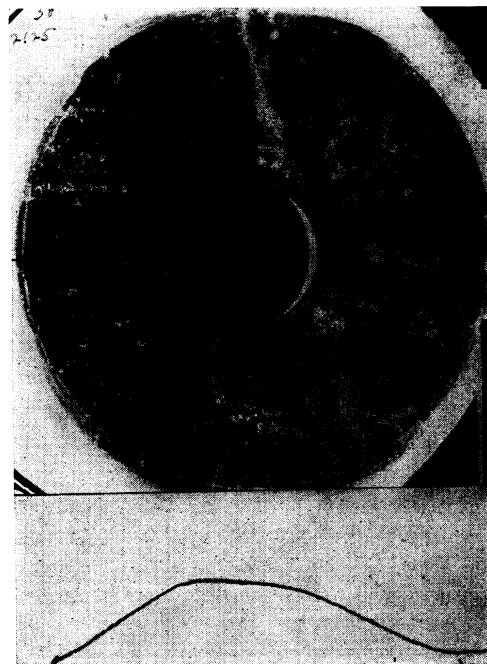


c



d

particle from the chamber wall. Table IV indicates that 42 percent of the nuclear disintegrations recorded by the ionization chamber (i.e., 36 out of 86) gives visible heavy tracks in the cloud chamber. Thus the 3-shower records must be compared with about 130 nuclear disintegrations in estimating the relative numbers of bursts produced by the two kinds of events. This comparison shows that only a very small fraction of the bursts in the unshielded ionization chamber are caused by showers, in agreement with the results obtained from the coincidence experiment described in Part III. When lead was placed either above the cloud chamber or directly on the ionization chamber, the number of elec-



e

FIG. 23. Correlated cloud-chamber-ion-chamber records. The series (a), (b), (c) are examples in which the cloud chamber shows one or more heavily ionizing tracks from the ion chamber. They have been selected to show the greatest variation encountered in pulse shape in cases where the pulse is the result of a nuclear disintegration. Most pulses under these conditions are similar to example (a). Except for a slight break hardly visible in the reproduction, (b) would be classified as σ -type. Example (c) is a ν -type pulse the slope of which decreases with time. The cloud chamber shows 11 heavily ionizing tracks. Examples (d) and (e) show electron showers which originate in a one inch lead plate on top of the cloud chamber. It is somewhat unexpected that even when the axis of the shower is as far to the side as in (e) a σ -pulse is still obtained.

TABLE IV. Correlation of ion-chamber and cloud-chamber records, giving the number of cases in which a given type of cloud-chamber picture was associated with a given type of ionization-chamber record.

	α	ν	σ	Total
No associated tracks	35	9	6	50
Heavy tracks from the ion chamber wall	29	7	0	36
Electron shower	0	0	12	12
Total	64	16	18	98

tron showers relative to the number of nuclear disintegrations increased markedly, as one should expect. About two-thirds of the showers observed under lead came from a single point in the lead, thus indicating that one electron or photon was responsible for the event observed in each case. In one-third of the cases there appeared to be several electrons or photons from an air shower incident upon the instrument and undergoing cascade multiplication in the lead shield.

4. Results Concerning Nuclear Disintegrations

We wish to discuss now in more detail the pictures of nuclear disintegrations. Table VI gives the distribution in size of nuclear disintegrations from the ionization-chamber wall observed at 3050 meters and 4300 meters, re-

TABLE V. Number of cloud chamber pictures showing nuclear disintegrations and electron showers under different experimental conditions.

Altitude	Lead shield	Event observed			
		Heavy tracks from ionization chamber	Showers from air	Showers from lead above cloud chamber	Showers from lead on ionization chamber
3050 m	none	21	1	—	—
3050 m	$\frac{1}{2}$ inch over cloud chamber	8	0	2*	—
3050 m	$\frac{1}{4}$ inch on ion chamber and $\frac{1}{2}$ inch on cloud chamber	1	2	1*	2
3050 m	$\frac{1}{4}$ inch on ion chamber	16	0	—	3
4300 m	none	34	2*	—	—
4300 m	1 inch above cloud chamber	54	9	15*	—

* One event in each case had a slow heavy particle coming from the ionization chamber wall as well as the electron shower component.

spectively. In the compilation of this table, the pictures obtained under various lead shields are all considered together. It appears that the character of the nuclear disintegrations does not change significantly between 3050 and 4300 meters. The results on the number-frequency distribution of disintegration particles obtained at the two altitudes have been combined and presented graphically in Fig. 24a. Figure 24b shows the corresponding frequency distribution of the events for which a simultaneous pulse shape record was available. In Fig. 24b the point at abscissa zero gives the number of events in which the ionization chamber detected a burst and no heavily ionizing track was visible in the cloud chamber.

We wish to underline some of the results obtained from the cloud-chamber observations.

(a) Most of the nuclear disintegrations were initiated by non-ionizing particles. Only a few percent of the pictures showed any lightly ionizing particles which could possibly be identified with the initiating particle, and some of these might actually have been produced in the disintegration. One thus concludes that nuclear absorption of negative mesons at the end of their range does not play an important role as a cause of disintegrations. The present data furnish further evidence that the non-ionizing particles which produce nuclear disintegrations are not photons, since, when lead was present above the chamber, photons would come out of the lead accompanied by electron showers (see also III.4, above).

(b) As already pointed out, about 42 percent of the nuclear disintegrations observed in the ionization chamber give rise to particles which appear in the corresponding cloud chamber pictures. Most of the disintegrations which give rise to ionization bursts take place within the wall of the ionization chamber and therefore the disintegration particles do not need to traverse the whole wall thickness to appear in the cloud-chamber volume. On the other hand, these particles, in general, do not come out at right angles to the surface of the ionization chamber. One thus estimates that the average range of the disintegration particles which appear in the cloud chamber is larger than the wall thickness ($\frac{1}{32}$ -inch brass). A range of $\frac{1}{32}$ -inch brass cor-

responds to an energy of 21 Mev for protons and to a higher energy for heavier particles. We thus conclude that almost one half of the disintegrations that give pulses larger than 6 Mev in the ionization chamber contain at least one particle of energy larger than 21 Mev. The average number of these particles with energy larger than 21 Mev is 1.8 per disintegration observed in the cloud chamber, 0.75 per disintegration observed in the ionization chamber. In the 17 pictures of nuclear disintegrations obtained with $\frac{1}{4}$ inch of lead above the ionization chamber there were 35 heavily ionizing particles observed in the cloud chamber, of which 4 came out of the ionization chamber through the lead shield. The energy of these particles, if protons, must have been greater than about 64 Mev.

(c) Fourteen of the 88 disintegrations observed at 4300 meters and one of the 49 observed at 3050 meters apparently showed time-associated heavy tracks passing through the gas in the cloud chamber. Time association was determined from the "width" of the tracks, which varies as $t^{\frac{1}{2}}$. From the known time rate of change of width and an estimate of $\frac{1}{2}$ mm for the accuracy of track width measurement, we obtain about $\pm 1/50$ sec. for the uncertainty in time simultaneity at a time corresponding to the chamber-triggering tracks. Thus, it seems unlikely that all of the above events can be explained as accidental coincidences of unrelated events although it is impossible to determine what fraction represents true time association from the present data. Figure 22a is an illustration of an event in which a disintegration in the ion chamber is apparently time-associated with a disintegration in the cloud-chamber wall. If one of the disintegrations was caused by a particle from the other disintegration, the connecting link, was a non-ionizing particle. It may be noted that the existence of time-associated nuclear disintegrations is strongly indicated by other observations.¹⁹ It can be explained either by the simultaneous arrival on the instrument of several particles (neutrons?) capable of producing nuclear disintegrations, or by the pro-

¹⁹ See, for example, J. Daudin, *Ann. de Phys.* **19**, 110 (1947); W. B. Fretter and W. E. Hazen, *Phys. Rev.* **70**, 230 (1946); H. Bridge and W. E. Hazen, *Phys. Rev.* **74**, 579 (1948).

TABLE VI. Distribution in size of the nuclear disintegrations.*

Number of particles per disintegration	Number of records	
	at 3050 m	at 4300 m
1	27	52
2	11	21
3	6	5
4	3	3
5	2	4
6	0	0
7	0	3
Total number of particles observed	89	160
Average number of particles per disintegration observed	1.8	1.8

* This table includes some additional data obtained at 3050 meters with 4 brass plates in the cloud chamber which are not included in Tables IV and V.

duction in nuclear disintegrations of secondary particles capable of producing more disintegrations. The mere existence of such effects is not surprising. Their rate of occurrence, however, when accurately known, may furnish very important clues as to the nature of the particles responsible for nuclear interactions and the order of multiplicity in their production. Experiments intended to investigate this question are in preparation.

5. Comparison with the Results of the Coincidence Experiment

As already noted, the cloud-chamber observations fully confirm the conclusion reached from the coincidence experiment, that, at mountain

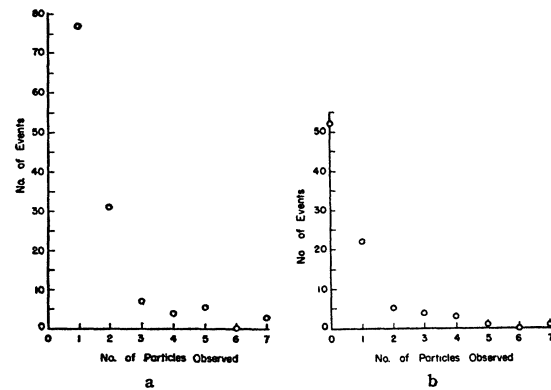


FIG. 24. (a) Number-frequency distribution for all cloud-chamber pictures in which heavily ionizing particles were observed. (b) Number-frequency distribution for cloud-chamber pictures correlated with pulse shape records. The point at zero abscissa indicates the number of events in which the ionization chamber gave a record characteristic of a nuclear disintegration and no heavily ionizing track was observed in the cloud chamber.

altitudes, all but a few percent of the ionization pulses in an unshielded chamber of our type are caused by nuclear disintegrations. These experiments also confirm the view that most of the coincidences between two neighboring chambers have the same origin, since they show that protons sufficiently energetic to traverse the chamber walls, yet sufficiently slow to ionize heavily, are produced very often in the nuclear disintegrations.

ACKNOWLEDGMENTS

The expedition at Climax was made possible by the cooperation of Mr. C. J. Abrams of the Climax Molybdenum Company and Drs. Walter

Orr Roberts and John W. Evans of the Harvard College Observatory. The B-29 used for the measurements at high altitudes was provided by the U. S. Air Force. For the work at Doolittle Ranch and Mt. Evans the authors were fortunate in having the assistance of Mr. R. J. Davisson and Mr. H. Courant. Professor Mario Iona of the University of Denver greatly facilitated the work of the Doolittle Ranch-Mt. Evans expedition. Janet R. Williams assisted in analyzing much of the data.

The cloud chamber was constructed during the tenure of a Guggenheim Fellowship. The work described was supported in part by the Office of Naval Research.

Sea Level Latitude Effect of Cosmic Radiation*†

PETER A. MORRIS, W. F. G. SWANN, AND H. C. TAYLOR

Bartol Research Foundation of the Franklin Institute, Swarthmore, Pennsylvania

(Received June 17, 1948)

On a recent voyage from Rio de Janeiro to Boston the vertical intensity of the total and hard components of the cosmic radiation were measured with a Geiger counter telescope apparatus. For the hard component the percentage alteration from high latitudes to the magnetic equator was 5.32 ± 0.46 percent. For the soft component it was 4.46 ± 0.61 percent, and for the total radiation it was 5.04 ± 0.55 percent.

I. INTRODUCTION

PREVIOUS measurements of the sea level latitude distribution of cosmic radiation have been made chiefly with ionization chambers, although some measurements have been made with coincidence counter systems. The use of counter systems allows the determination of the effect for the soft component of the radiation either by noting the relationship between the soft component and showers produced in small thickness of lead, or by taking the differences between the intensities of the total and hard components. The extensive measurements by Compton and Turner¹ and by Gill,² for example,

were obtained by using the ionization chamber method. Coincidence counter measurements have been made by Auger and Leprince-Ringuet,³ Clay, Bruins and Wiersma,⁴ Johnson and Read,⁵ Wilson and Turner,⁶ and Neher and Pickering.⁷ According to Johnson,⁸ the agreement between the two methods has been good, taking into account the fact that one might expect a somewhat greater latitude effect for the vertical intensities (measured by coincident counter systems) than for the integrated directional meas-

² P. S. Gill, *Phys. Rev.* **55**, 1151 (1939).

³ P. Auger and L. Leprince-Ringuet, *Comptes Rendus* **197**, 1242 (1933); P. Auger, *Nature* **133**, 138 (1934).

⁴ J. Clay, E. M. Bruins, and J. T. Wiersma, *Physica* **3**, 746 (1936).

⁵ T. H. Johnson and D. N. Read, *Phys. Rev.* **51**, 557 (1937).

⁶ V. C. Wilson and R. N. Turner, *Phys. Rev.* **59**, 931 (1941).

⁷ H. V. Neher and W. H. Pickering, *Phys. Rev.* **53**, 111 (1938).

⁸ T. H. Johnson, *Rev. Mod. Phys.* **10**, 193 (1938).

* Assisted by the Office of Naval Research with the cooperation of the National Geographic Society.

† A skeleton of the results of this investigation has been published in *Phys. Rev.* **72**, 1263 (1947).

¹ A. H. Compton and R. N. Turner, *Phys. Rev.* **51**, 1005 (1937); **52**, 799 (1937).

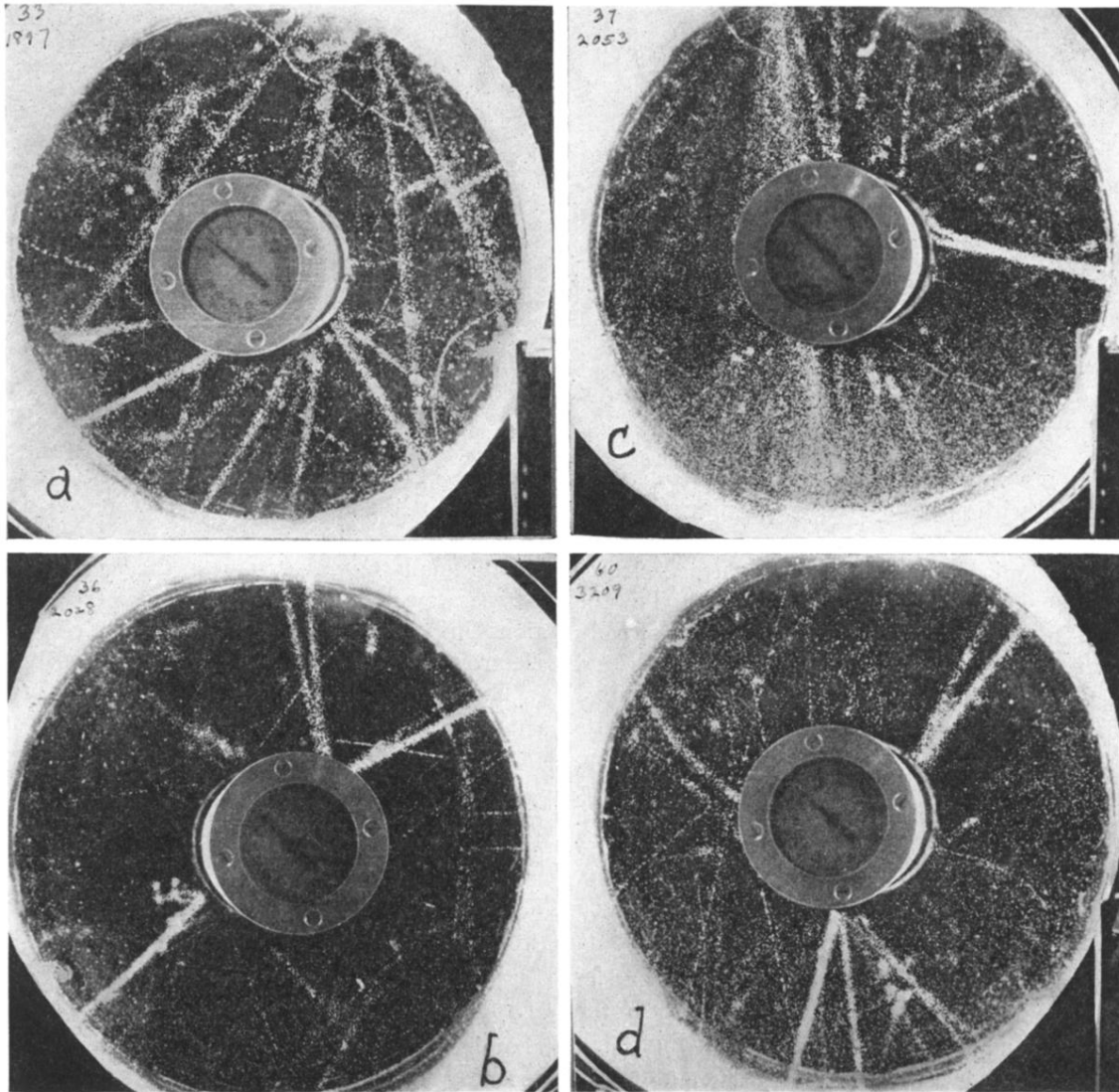
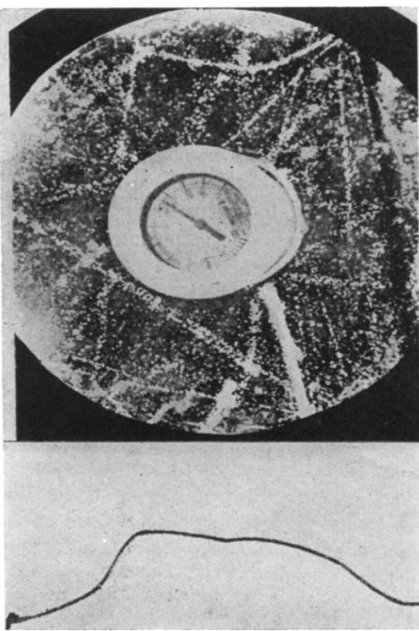
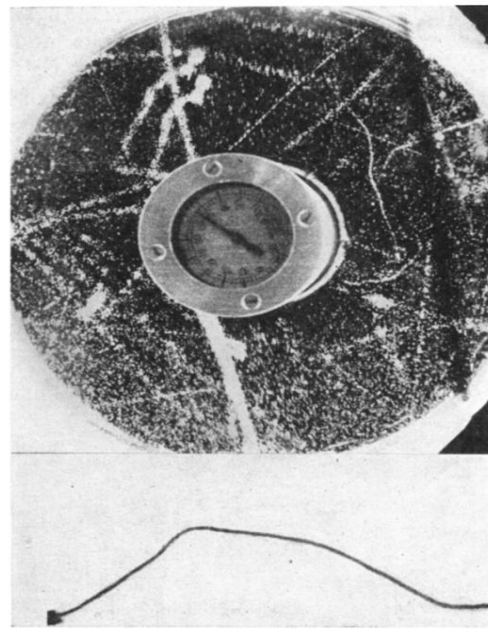


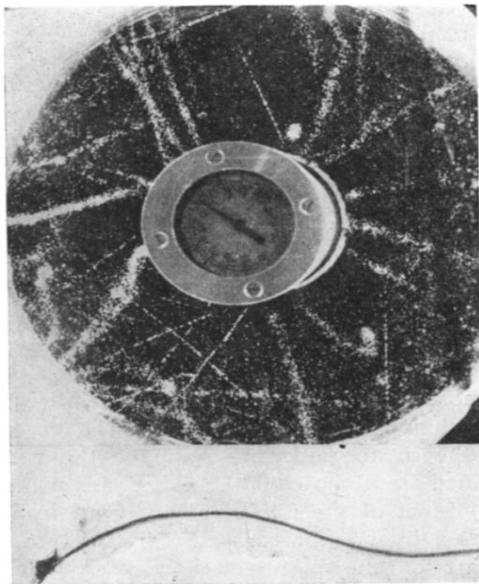
FIG. 22. Example of the cloud-chamber pictures. (a) An event in which a disintegration in the cloud-chamber wall is concurrent with a disintegration in the ionization-chamber wall. The latter may be initiated by a neutron from the former or both may be produced by neutrons from a disintegration above the apparatus. (b) A disintegration with four heavily ionizing and one lightly ionizing particles. (c) An electron shower from lead above the chamber apparently produces at least two heavy particles in a disintegration in the ionization-chamber wall. (d) A disintegration with at least seven particles appearing in the cloud chamber.



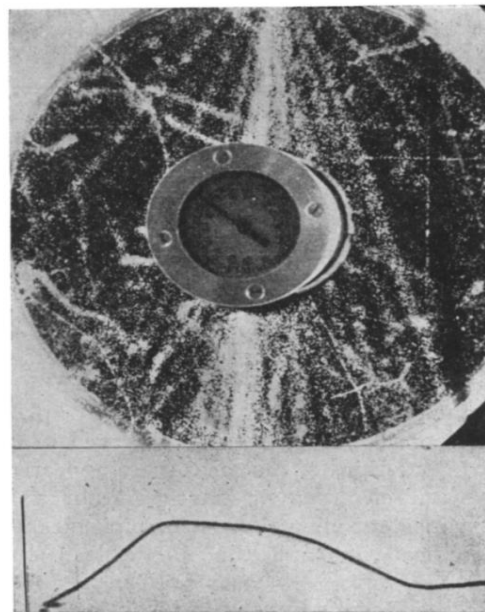
a



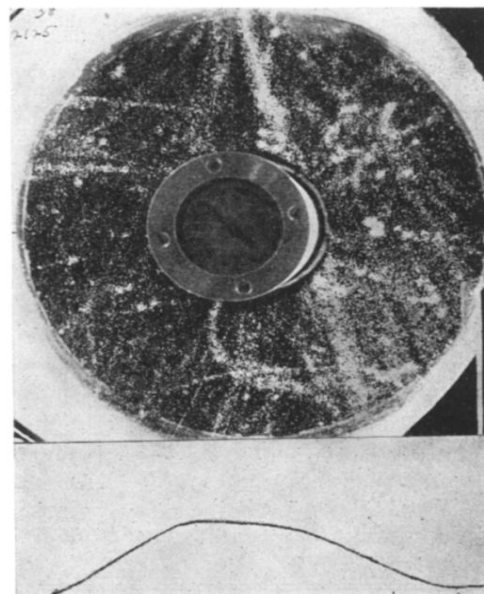
b



c



d



e

FIG. 23. Correlated cloud-chamber-ion-chamber records. The series (a), (b), (c) are examples in which the cloud chamber shows one or more heavily ionizing tracks from the ion chamber. They have been selected to show the greatest variation encountered in pulse shape in cases where the pulse is the result of a nuclear disintegration. Most pulses under these conditions are similar to example (a). Except for a slight break hardly visible in the reproduction, (b) would be classified as σ -type. Example (c) is a ν -type pulse the slope of which decreases with time. The cloud chamber shows 11 heavily ionizing tracks. Examples (d) and (e) show electron showers which originate in a one inch lead plate on top of the cloud chamber. It is somewhat unexpected that even when the axis of the shower is as far to the side as in (e) a σ -pulse is still obtained.

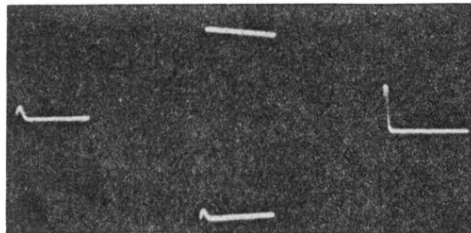


FIG. 9. Photographic record of the four horizontal traces of the coincidence method. The apparatus was triggered by the large pulse appearing on the right-hand trace; two other traces show small time-coincident pulses.